ORIGINAL CONTRIBUTION

Preparation and properties of natural rubber with filler nanomatrix structure

Nurul Hayati Yusof[1,2] · Kenshi Noguchi[1] · Lina Fukuhara[3] · Yoshimasa Yamamoto[3] ·
Seiichi Kawahara[1]

Abstract Natural rubber with filler nanomatrix structure was prepared by forming chemical linkages between natural rubber particles and filler nanoparticles. The filler nanomatrix structure was formed by graft copolymerization of vinyltriethoxysilane (VTES) onto natural rubber particles in the latex stage followed by casting of the latex to prepare an as-cast film. The silica nanoparticles were produced during the graft copolymerization through hydrolysis and condensation, i.e., sol–gel reaction; hence, they linked to the natural rubber particles. The nanomatrix structure was observed by transmission electron microscopy, in which the natural rubber particles of about 1 μm in diameter were well dispersed in the filler nanomatrix. Tensile properties were significantly improved by forming filler nanomatrix structure. The loss modulus and loss tangent of the natural rubber with the filler nanomatrix structure were almost independent of deformation frequency in the rubbery plateau region, which was explained to be due to the energetic elasticity and entropic elasticity characteristic of the nanomatrix structure.

Keywords Natural rubber · Filler nanomatrix · Silica nanoparticle · TEM · Mechanical properties

✉ Seiichi Kawahara
kawahara@mst.nagaokaut.ac.jp

[1] Department of Materials Science and Technology, Faculty of Engineering, Nagaoka University of Technology, Nagaoka, Niigata 940-2188, Japan

[2] Malaysian Rubber Board, RRIM Research Station, Sg. Buloh, 47000 Selangor, Malaysia

[3] Department of Chemical Science and Engineering, Tokyo National College of Technology, 1220-2, Kunugida-machi, Hachioji, Tokyo 193-0997, Japan

Introduction

Filler nanomatrix structure is a novel nanostructure of nanocomposites, which may greatly contribute to the outstanding mechanical properties. Here, the filler nanomatrix structure is defined as a nanostructure consisting of organic particles as the major component and inorganic matrices as the minor component. Thus, natural rubber with a filler nanomatrix structure may consist of natural rubber particles of about 1 μm in diameter and filler nanoparticles of about several nanometers in diameter, in which the filler nanoparticles are chemically linked to the natural rubber particles [1]. It is expected that the remarkable mechanical properties, required for high-performance applications, can be realized by the filler nanomatrix structure.

The formation of the filler nanomatrix structure may be concerned with the method to control the morphology [2–4]. The filler nanomatrix structure may be formed by graft copolymerization of functional organosilane monomer onto NR in the latex stage followed by coagulation. The silica nanoparticles are formed by condensation during drying after the graft copolymerization, which may form strong chemical linkages with the natural rubber particles. This may result in the unique properties of rubbery polymers, since the filler nanomatrix structure is distinguished from the ordinary island-matrix structure, which is usually formed by blending polymer with filler [5–8].

The filler effects on the properties of the filled rubber are comprised of three important factors, which are (1) volume effect, (2) interface effect, and (3) cavitation effect. The volume effect is proportional to the volume fraction of the filler, while the interface effect is related to the interactions between the rubber and the filler, and the cavitation effect depends on the presence of an interfacial cavity or void between the rubber and the filler. The volume effect and the interface effect

may play important roles in improving and reinforcing properties of the filled rubber. On the other hand, the cavitation effect reduces the properties because of the propagation of the generated cracks. Besides, the morphology also can influence the properties of the filled rubber. Since each effect has a unique origin, therefore, it is necessary to comprehend these factors [9–11].

Furthermore, the relationships between the polymer–polymer interaction, polymer–filler interaction, and filler–filler interaction [12–14] have to be considered. Figure 1 shows a schematic illustration of filler network. The polymer–polymer interaction represents the chain entanglement network, i.e., CeN; the polymer–filler interaction represents the bridged filler network, i.e., BFN; and the filler–filler interaction represents the contact filler network, i.e., CFN. When the simple model is considered, a stress of the filled rubber may be expressed as a linear combination of stresses of the CeN, BFN, and CFN [15].

The logarithmic horizontal shift factor, $\log a_T$, is dependent upon temperature, while being independent of the filler content [15]. The a_T was well expressed by the WLF equation [16–18], even after loading the fillers. The WLF Eq. (1) is expressed by the following equation:

$$\log a_T = \frac{-C_1(T-Tg)}{C_2 + T - Tg} \tag{1}$$

In the case of rubber, the segment as a hard sphere is dispersed in the matrix. The a_T is, thus, expressed by the following Eq. (2):

$$\log a_T = \log \frac{\tau_i(T)}{\tau_i(T_r)} = \log \frac{\eta_i(T)}{\eta_i(T_r)} = \log \frac{\eta_{local}(T)}{\eta_{local}(T_r)}$$
$$= \log \frac{\xi_{segment}(T)}{\xi_{segment}(T_r)} \tag{2}$$

Similarly, in the case of filled rubber, the filler as a hard sphere is dispersed in the rubber matrix. The a_T is, thus, expressed by this Eq. (3):

$$\log a_T = \log \frac{\xi_{filler}(T)}{\xi_{filler}(T_r)} = \log \frac{\eta_{matrix}(T)}{\eta_{matrix}(T_r)}$$
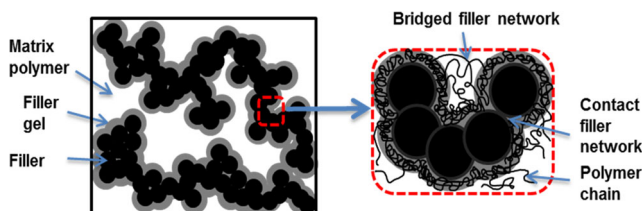$$= \log \frac{\xi_{segment}(T)}{\xi_{segment}(T_r)} \tag{3}$$

Fig. 1 Schematic illustration of filler network

Consequently, the horizontal shift factor for rubber must be the same as that for the filled rubber. In contrast, the vertical shift factor, b_T, is dependent upon the filler content. The b_T is known to be proportional to temperature [15, 19]. Thus, the b_T must increase as the temperature increases. The monotonic increase in the b_T is found for SBR/carbon black 0 phr and SBR/carbon black 20 phr. However, the slope of the b_T versus temperature changed from positive to negative, when the carbon black content increased. The negative slope may be explained to be due to the effect of the filler–filler interaction, since elasticity may be divided into two contributions, that is, entropic elasticity and energetic elasticity. It is worthy of note that the entropic elasticity is completely distinguished from the energetic elasticity [15].

In order to achieve not only entropic elasticity but also energetic elasticity, simultaneously, a specific nanostructure may be formed. It may be composed of dense nanofiller portion and less nanofiller portion. One of the plausible structures is the filler nanomatrix structure, which consists of natural rubber particles and the nanoparticles of the filler. The nanoparticles gather together to form the nanomatrix and the natural rubber particles are dispersed in the nanomatrix. The natural rubber particles may generate the entropic elasticity whereas the nanomatrix may generate the energetic elasticity. In this case, the entropic elasticity and energetic elasticity may stand together.

The aim of the present study is to realize both the energetic elasticity and entropic elasticity of a soft material, from the preparation of natural rubber with organosilane monomer. An attempt to prepare natural rubber with organic–inorganic nanomatrix structure was performed by graft copolymerization of vinyltriethoxysilane (VTES) followed by hydrolysis and condensation. Morphology of the resulting graft copolymer was observed by transmission electron microscopy. The mechanical properties such as the tensile properties and the viscoelastic properties were measured, as well.

Materials and methods

High ammonia natural rubber (HANR) latex was purchased from Golden Hope Plantation, Malaysia. The surfactant of sodium dodecyl sulfate (SDS); *tert*-butylhydroperoxide (TBHP), 68 %; and tetraethylenepentamine (TEPA) were from Kishida Chemicals (Japan). Urea was from Nacalai Tesque (Japan). Vinyltriethoxysilane (VTES) was from Chisso Kabushiki Company (Japan). The solvents such as acetone, tetrahydrofuran (THF), methanol, and toluene used were of industrial grade from Nacalai Tesque (Japan).

Removal of proteins from natural rubber latex

The removal of the proteins from the high ammonia natural rubber (HANR) latex was carried out by incubation of the latex with urea in the presence of SDS. The HANR latex was firstly diluted from $60 w/w\%$ dry rubber content (DRC) with distilled water to $30 w/w\%$ of DRC before use. The amounts of urea ($0.1 w/w\%$) and SDS ($1.0 w/w\%$) were added into the latexes. The latexes were, then, centrifuged (~10,000g) three times at 288 K for 30 min. The cream fraction was collected after the second and third centrifugation and was re-dispersed in the solution with $0.5 w/w\%$ SDS and $0.1 w/w\%$ SDS, respectively. Finally, the SDS concentration of the resulting deproteinized natural rubber (DPNR) latex was adjusted to $0.1 w/w\%$. The percentage of urea and SDS used in this preparation was based on the overall solution. Prior to the graft copolymerization, DPNR latex was diluted to $20 w/w\%$ DRC and topped up with $0.5 w/w\%$ SDS.

Preparation of graft copolymerization

The graft copolymerization of the DPNR latex was carried out with vinyltriethoxysilane (VTES) monomer, using TBHP and TEPA as initiators. The DPNR latex of 200 g with $20 w/w\%$ DRC and $0.5 w/w\%$ SDS was purged with N_2 gas in the reaction flask, for 1 h. Then, the initiator and monomer were added in sequence to the latex. The reaction was performed for 2 h with continuous stirring at 200 rpm under N_2 atmosphere at 303 K in water bath. The un-reacted monomer was removed from the gross polymer with a rotary evaporator under reduced pressure for about 30 min at 353 K. The reacted latex was poured into a petri dish and dried in the oven at 323 K for about 2 days (until dry) and in a vacuum oven for 3 days at 323 K. Conditions for the graft copolymerization of the DPNR latex with VTES are shown in Table 1.

Preparation of DPNR-*blend*-silica

Colloidal silica (Snow Tex XS) was mixed with $10 w/w\%$ ethanol aqueous solution. Then, the mixture was poured into DPNR latex and stirred homogeneously. The DPNR-*blend*-silica was cast as a film and dried under reduced pressure at 323 K.

Material characterizations

The surface topography was observed with a scanning probe microscope (SPM-9500 J3), Shimadzu, Kyoto, Japan. The observation was carried out at 298 K and at a magnification of ×1000.

Observation of morphology at high magnification was done by transmission electron microscopy (TEM, JEOL JEM-2100) at an accelerating voltage of 200 kV. The ultra-thin sections of the sample were prepared by a Richert-Nissei FC S-Ultracut at a temperature of 183 K. The thin cut sections then were placed onto the copper grid before being subjected to the electron beam of the TEM.

Measurements of the tensile properties were carried out according to JIS K6251. The film samples with thickness of about 1 mm were cut with a Dumbell-shaped Type 7. The test piece was stretched with the speed rate of 200 mm/min. Data of the stress and strain of the sample were plotted in a stress–strain curve.

The dynamic viscoelasticity was measured with an Anton Paar Physica MCR 301. Parallel plate geometry of 12-mm diameter was used. Angular frequency range was from 0.1 to 100 rad/s. Temperature range was from 203 to 413 K. The oscillatory strain amplitudes were within the range of the linear viscoelasticity in all measurements.

Results and discussion

Graft copolymerization of vinyltriethoxysilane (VTES)

Figure 2 shows the conversion and grafting efficiency of vinyltriethoxysilane (VTES) in the latex stage at various initiator concentrations, i.e., (a) 3.3×10^{-2} and (b) 6.6×10^{-2} mol/kg rubber. The conversion and grafting efficiency of the VTES were estimated from the mole ratio of resulting polymer to the fed monomer, and the mole ratio of the grafted polymer to the resulting polymer, respectively, as in the following expressions:

$$Conversion(mol\%) = \frac{Amount\ of\ PVTES\ in\ gross\ polymer}{Amount\ of\ fed\ VTES\ monomer} \times 100$$

$$Gratf\ Efficiency\ (mol\%) = \frac{Amount\ of\ PVTES\ in\ grafted\ polymer}{Amount\ of\ PVTES\ in\ reacted\ polymer} \times 100$$

The conversion of VTES at the initiator concentration of 3.3×10^{-2} mol/kg rubber decreased as the monomer concentration increased, whereas the grafting efficiency increased, as shown in Fig. 2a. The decrease in the conversion may be explained to be due to the excess amounts of VTES as compared with the initiator concentration. In contrast, the increase in the grafting efficiency may suggest that the active sites for the graft copolymerization dominantly exist on the natural rubber particles, but not in the water phase (serum); hence, the homo-polymerization may be suppressed.

In Fig. 2b, at the initiator concentration of 6.6×10^{-2} mol/kg rubber, the conversion was about 97 mol%, and it was independent of the monomer concentration. The high conversion implies that the initiator concentration is highly sufficient for the polymerization of VTES. In contrast, the grafting efficiency was dependent upon the monomer concentration, that is, the higher the monomer concentration, the higher the grafting efficiency. The low grafting efficiency may be

Table 1 Conditions of graft copolymerization of DPNR latex with VTES monomer

Sample name	DRC (*w/w*%)	Initiator (mol/kg rubber)	Monomer (mol/kg rubber)	Reaction time (h)	Reaction temperature (K)
VTES-3.3-0.5	20	3.3×10^{-2}	0.5	2	303
VTES-6.6-0.5	20	6.6×10^{-2}	0.5	2	303
VTES-3.3-1.05	20	3.3×10^{-2}	1.05	2	303
VTES-6.6-1.05	20	6.6×10^{-2}	1.05	2	303
VTES-3.3-1.5	20	3.3×10^{-2}	1.50	2	303
VTES-6.6-1.5	20	6.6×10^{-2}	1.50	2	303

attributed to the excess amounts of initiator as compared to the monomer concentration. The initiator may exist not only on the surface of the rubber particles but also in the water phase, in which the initiator in the water phase may react with the monomer to form homo-polymer. The increase in the grafting efficiency with the increase of the monomer concentration may be explained to be due to a suitable ratio of the monomer concentration to the initiator concentration. The initiator may be dominantly used to generate the active sites on the surface of the natural rubber particles. Thus, in the present study, the suitable initiator concentration, i.e., *tert*-butylhydroperoxide (THBP) and tetraethylenepentamine (TEPA), is found to be 6.6×10^{-2} mol/kg rubber for the graft copolymerization of vinyltriethoxysilane (VTES) onto natural rubber at 303 K.

Scanning probe microscope images

Figure 3 shows the scanning probe microscope (SPM) images for VTES-6.6-0.5, VTES-6.6-1.05, and VTES-6.6-1.50. The hardness on the surface of the film was distinguished by color contrast; for instance, the dark domains represent the rigid phase while the bright domains represent the soft phase. As for VTES-6.6-0.5, the bright particles of about 1 μm in average diameter were well dispersed in the nanomatrix of about several tens of nanometers in thickness. Furthermore, in the nanomatrix, the small dark particles were found to be

dispersed, closely. As the monomer concentration increased, the small dark particles were distinctly found in the nanomatrix, for instance, in VTES-6.6-1.05 and VTES-6.6-1.50. Hence, the hardness on the surface of the film was dependent upon the monomer concentration at the initiator concentration of 6.6×10^{-2} mol/kg rubber, in which the higher the monomer concentration, the harder the surface of the film.

In the recent work [1], it was reported that the highest value of stress at break was achieved at 1.05 mol/kg rubber of monomer concentration. The value of stress at break was about three times as high as that of the DPNR (5 MPa). Thus, the graft copolymer, prepared with the 1.05 mol/kg rubber monomer and 6.6×10^{-2} mol/kg rubber initiator, will be characterized in the subsequent section.

Transmission electron microscopeimages

Figure 4 shows the transmission electron microscope (TEM) images for DPNR and VTES-6.6-1.05. In the TEM images (unstained), the bright domains represent natural rubber, and the dark domains represent silica nanoparticles. The silica nanoparticles, which were about 10–150 nm in diameter, were aligned along with the rubber particles, as shown in Fig. 4b. Between the rubber particles and silica nanoparticles, the vinyl polymers (thin gloomy line) were expected to form in order to link the rubber particles to the silica nanoparticles. The rubber
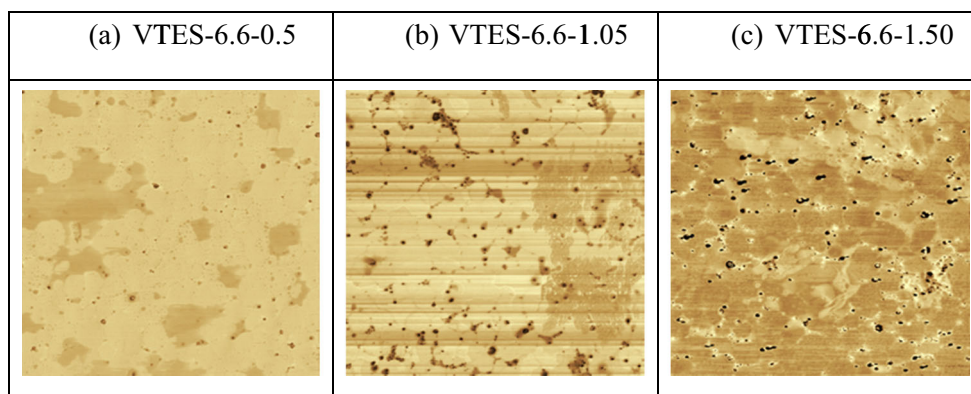
Fig. 2 Conversion (mol%) and grafting efficiency (mol%) of VTES at the initiator concentration of (**a**) 3.3×10^{-2} and (**b**) 6.6×10^{-2} ranging from 0.5 to 1.50 mol/kg rubber
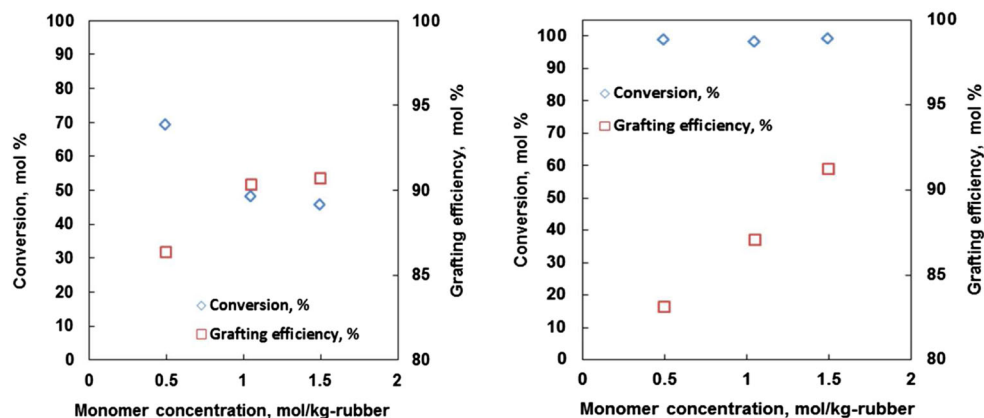
(a) Initiator: 3.3 ×10⁻² mol/kg-rubber

(b) Initiator: 6.6 ×10⁻² mol/kg- rubber

Fig. 3 Surface morphology observed by SPM for (**a**) VTES-6.6-0.5, (**b**) VTES-6.6-1.05, and (**c**) VTES-6.6-1.50

| (a) VTES-6.6-0.5 | (b) VTES-6.6-**1**.05 | (c) VTES-6.6-1.50 |

particles were well dispersed in the nanomatrix of several tens of nanometers in thickness, consisting of silica nanoparticles and vinyl polymers, as shown in Fig. 4c. The vinyl polymers were considered to be polymer fragments obtained by the graft copolymerization of vinyltriethoxysilane, while silica nanoparticles were realized by the hydrolysis and condensation of vinyltriethoxysilane.

Storage modulus

Figure 5 shows the storage modulus (G') at the rubbery plateau region versus the frequency for the DPNR and VTES-6.6-1.05. The value of the storage modulus at the plateau region for the DPNR was about 10^5 Pa, which was similar to that reported in previous literatures [20, 21]. When the filler nanomatrix structure was formed in natural rubber, i.e., VTES-6.6-1.05, the storage modulus increased about two times as high as that of the DPNR. The increase in the storage modulus at the plateau region for VTES-6.6-1.05 was quite similar to that of the DPNR with the nanomatrix of polystyrene (PS), which was about 3.5 times as high as that of the DPNR as reported in previous literature [22].

Loss modulus

Figure 6 shows the loss modulus (G'') at the plateau region versus the frequency for the DPNR and VTES-6.6-1.05. The

loss modulus at the plateau region for the DPNR decreased as the frequency increased, in which the higher the frequency, the lower the loss modulus. In contrast, the loss modulus at the plateau region for VTES-6.6-1.05, i.e., the DPNR with the filler nanomatrix structure, was found to be independent of the frequency; the loss modulus was almost constant as the frequency increased. The energy dissipation of VTES-6.6-1.05 may appear to be independent of the frequency. This is significantly distinguished from the relationship of the loss modulus and the frequency for the rubber and ordinary filled rubber. Hence, this finding is one of the remarkable properties of the filler nanomatrix structure.

Loss tangent

Figure 7 shows the loss tangent, tan δ versus the frequency, at the rubber plateau region for the DPNR and VTES-6.6-1.05. The value of tan δ for natural rubber is known to be in a range of 0.1 to 0.15, and it decreases at the plateau region as the frequency increases, as reported in previous literatures [20, 21]. The decrease in the value of tan δ versus the frequency was confirmed for the DPNR; the higher the frequency, the lower the value of tan δ. On the other hand, the value of tan δ for VTES-6.6-1.05 decreased at the low-frequency region and increased to almost constant at the high-frequency region. Therefore, in order to elucidate the relationship between viscoelastic properties and the filler nanomatrix structure, the

Fig. 4 TEM images for (**a**) DPNR (10 K × magnification), (**b**) VTES-6.6-1.05 (20 K × magnification), and (**c**) VTES-6.6-1.05 (10 K × magnification)

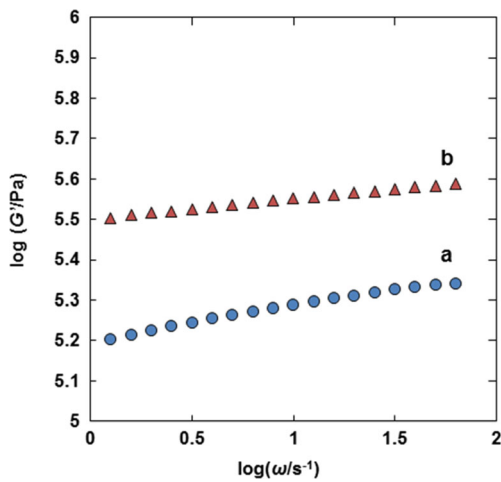| (a) DPNR (10K) | (b) VTES-6.6-1.05 (20K) | (c) VTES-6.6-1.05 (10K) |
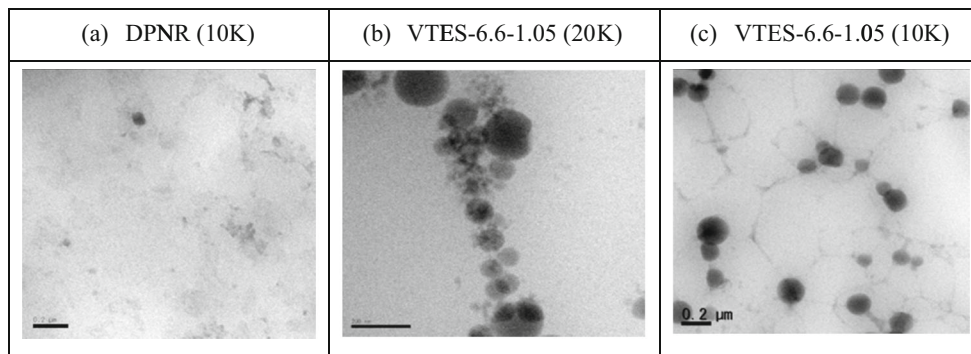
Fig. 5 Storage modulus (G') at plateau region versus frequency for (**a**) DPNR and (**b**) VTES-6.6-1.05

dependence of the viscoelastic properties on temperature and frequency was investigated.

Horizontal shift factor, a_T

Tan δ is useful to determine the horizontal shift factor, a_T, since it is defined as a ratio of loss modulus to storage modulus. The effects of temperature and density on the a_T may be eliminated, as long as the tan δ is used. Thus, in order to determine the horizontal shift factor, a_T, the tan δ in the plot of loss tangent versus frequency at various temperatures was horizontally superposed with the a_T to make a master curve, where the reference temperature, T_r, used was 215.5 K. The reference temperature, T_r, was selected in the plot of loss modulus (G'') versus the frequency at various temperatures of VTES-6.6-1.05.

The temperature dependency of a_T for the DPNR, DPNR-*blend*-silica, VTES-6.6-1.05 is shown in the Fig. 8, where the
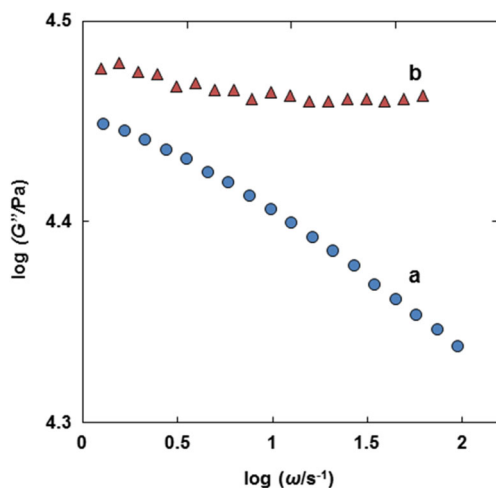

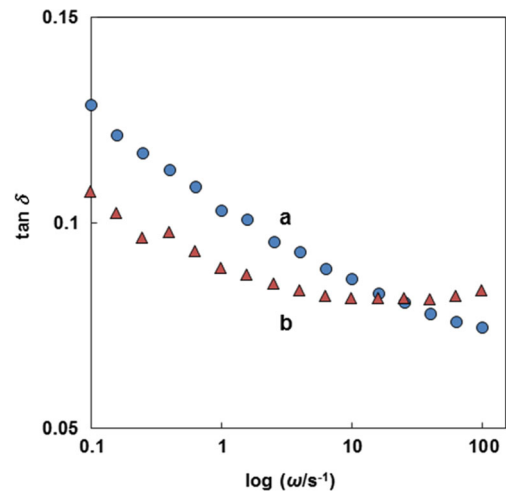**Fig. 6** Loss modulus (G'') at plateau region versus frequency for (**a**) DPNR and (**b**) VTES-6.6-1.05

Fig. 7 Loss tangent (tan δ) at plateau region versus frequency for (**a**) DPNR and (**b**) VTES-6.6-1.05

dotted line is estimated by a WLF equation for the DPNR and DPNR-*blend*-silica, and the broken line is estimated by a WLF equation for VTES-6.6-1.05. As mentioned in the "Introduction" section, the value of log a_T of pure rubber and filled rubber was in good agreement with that estimated by the WLF equation for pure rubber. This implies that the a_T is extensively dependent upon the relaxation behavior of the matrix polymer.

Vertical shift factor, b_T

Figure 9 shows the temperature dependency of the vertical shift factor—log b_T for the DPNR and VTES-6.6-1.05. As the silica nanoparticles are densely dispersed in the nanomatrix, the filler–filler and the filler–polymer interactions determine the energetic elasticity, whereas the rubber elasticity specifies the entropic elasticity. This elasticity is well expressed by the b_T, i.e., a negative value for the energetic elasticity and a positive value for the entropic elasticity. In
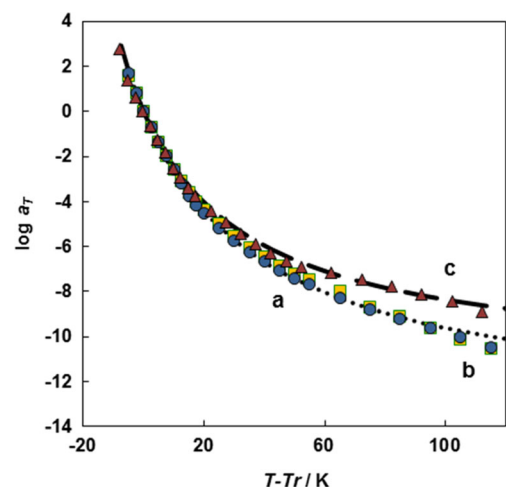

Fig. 8 Plot of horizontal shift factor (log a_T) versus temperature for (**a**) DPNR, (**b**) DPNR-*blend*-silica, and (**c**) VTES-6.6-1.05
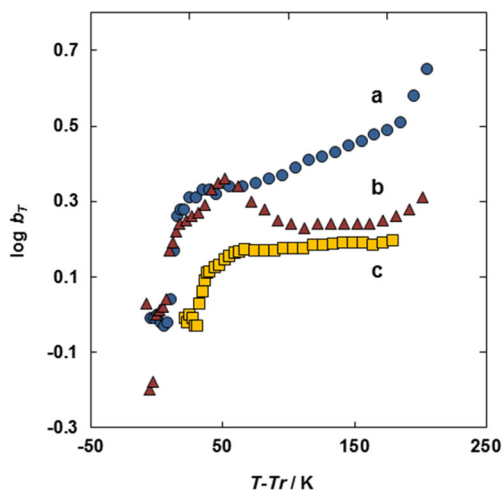
Fig. 9 Plot of vertical shift factor (log b_T) versus temperature for (**a**) DPNR, (**b**) VTES-6.6-1.05, and (**c**) DPNR-*blend*-silica

the Fig. 9, the log b_T for the DPNR increased linearly with the increasing temperature. This may represent the elasticity behavior of the pure natural rubber, where entropic elasticity occurs. The log b_T for DPNR-*blend*-silica was slightly increased as the temperature increased, suggesting the entropic elasticity, in which the elasticity behavior of the rubber is still dominant even though in the presence of silica particles. In the case of VTES-6.6-1.05, the vertical shift factor, b_T, initially increased until about 50 K and slightly decreased with the increasing temperature. This may be explained to be due to the energetic elasticity, which may be contributed by the presence of dense silica nanoparticles as a nanomatrix.

Since DPNR-*graft*-PVTES and DPNR-*blend*-silica consist of silica particles distributed in natural rubber matrix, the b_T for DPNR can be subtracted from b_T for VTES-6.6-1.05 and DPNR-*blend*-silica, respectively, in order to observe the energetic elasticity. Figure 10 shows the subtraction of b_T for DPNR from VTES-6.6-1.05 and DPNR-*blend*-silica. The b_T value for VTES-6.6-1.05 was negative, and it decreased with
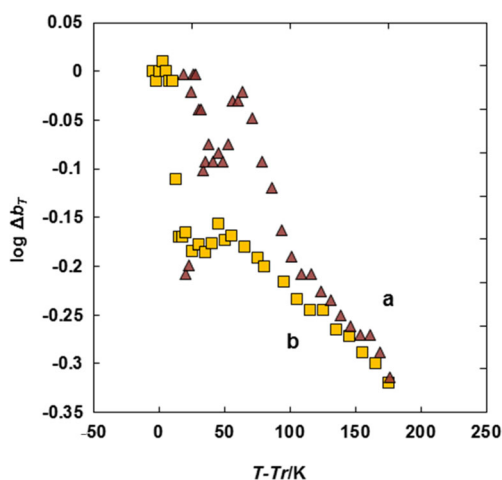
increasing temperature. In the case of DPNR-*blend*-silica, the b_T also showed a negative value, and it gradually decreased with increasing temperature. The decrease in b_T for VTES-6.6-1.05, compared to DPNR-*blend*-PVTES, may be explained to be due to the effect of nanomatrix. Consequently, this filler nanomatrix structure realizes both energetic elasticity and entropic elasticity.

Conclusions

Natural rubber with the filler nanomatrix structure was prepared by graft copolymerization of vinyltriethoxysilane onto natural rubber in the latex stage with 6.6×10^{-2} mol/kg rubber initiator, i.e., *tert*-butylhydroperoxide and tetraethylenepentamine, at 303 K. The conversion of vinyltriethoxysilane was about 97 mol% and the grafting efficiency was about 87 mol%. Almost all triethoxysilyl groups were converted to amorphous silica through the sol–gel reaction. The natural rubber particles of about 1 μm in average diameter were well dispersed in the silica nanomatrix, consisting of silica nanoparticles and vinyl polymer, as is evident from the TEM images. The mechanical properties of the natural rubber were significantly improved by the formation of the silica nanomatrix structure; for instance, the values of the loss modulus increased. The locus of the loss tangent delineated the concave curve. The unique viscoelastic properties were analyzed with horizontal and vertical shift factors. Entropic elasticity and energetic elasticity were realized in the filler nanomatrix structure.

Fig. 10 Subtraction of b_T for DPNR (**a**) from b_T for VTES-6.6-1.05 and (**b**) from b_T for DPNR-*blend*-silica

References

1. Kawahara S, Nurul Hayati Y, Noguchi K, Kosugi K, Yamamoto Y (2014) Organic inorganic nanomatrix structure and properties of related naturally occurring rubbery macromolecules. Polymer 55: 5024–5027

2. Pukkate N, Kitai T, Yamamoto Y, Kawazura T, Sakdapipanich J, Kawahara S (2007) Nano-matrix structure formed by graft-copolymerization of styrene onto natural rubber. Eur Polym J 43(8):3208–3214

3. Kawahara S, Yamamoto Y, Fujii S, Isono Y, Niihara K, Jinnai H, Nishioka H, Takaoka A (2008) FIB-SEM and TEMT Observation of highly elastic material with nanomatrix structure. Macromolecules 41:4510–4513

4. Kawahara S, Chaikumpollert O, Akabori K, Yamamoto Y (2011) Morphology and properties of natural rubber with nanomatrix of non-rubber components. Polym Adv Technol 22(12):2665–2667

5. Roland CM, Trask SA (1989) Miscible elastomer mixtures. Rubber Chem Technol 62(5):896–907

6. Joseph CS (1996) The Polymeric Materials Encyclopedia; Akiyama, S., Kawahara, S. CRC Press, pp 699–706

7. Tinker AJ, Jones KP (1998) Blends of natural rubber. Chapman & Hall, Berlin

8. Sam C, Nigel C (2014) Pattern formation in polymer blend thin films: surface roughening couples to phase separation. Phys Rev Lett 113:218301

9. Kawahara S, Yamamoto Y, Isono Y (2014) Controlling the performance of filled rubber. Nihon Reoroji Gakkaishi 42(2):79–88

10. Ivanov Y, Valerii C, Margarita N (2001) Polymer Composite Materials: Interface Phenomena & Processes, Solid Mechanics and Its Applications. Vol. 90. Kluwer Academic Publishers

11. Deepalekshmi P, Sabu T (2014) Non-Linear Viscoelasticity of Rubber Composites and Nanocomposites; Influence of Filler Geometry and Size in Different Length Scale. Springer International Publishing

12. Edwards DC (1990) Polymer-filler interactions in rubber reinforcement. J Mater Sci 25(10):4175–4185

13. Meng-Jiao W (1998) Effect of polymer-filler and filler-filler interactions on dynamic properties of filled vulcanizates. Rubber Chem Technol 71(3):520–589

14. Brechet Y, Cavaille JY, Chabert E, Chazeau L, Dendievel R, Flandin L, Gauthier C (2001) Polymer based nanocomposites: effect of filler-filler and filler-matrix interactions. Adv Eng Mater 3(8):571–577

15. Isono Y, Aoyama T (2013) Filler effects on temperature shift factors in viscoelastic properties of carbon black filled rubbers. Nihon Reoroji Gakkaishi 41(3):137–144

16. Ferry JD (1980) Viscoelastic properties of polymers. John Wiley & Sons

17. Lawrence EN, Robert FL (1994) Mechanical Properties of Polymers and Composites, 2nd ed.; Marcel Dekker, Inc

18. James EM (2007) Physical Properties of Polymers Handbook, 2nd ed.; Chapter 26: Temperature Dependences of the Viscoelastic Response of Polymer Systems; Springer, pp 455–478

19. Maghami S, Dierkes WK, Tolpekina TV, Schultz SM, Noordermeer JWM (2011) Presented at the Fall 180th Technical Meeting of the Rubber Division of the American Chemical Society, Inc. Cleveland

20. Brandrup J, Emmergut EH, Grulke EA (1998) Polymer Handbook, 4th ed.; V: Physical Constants of Some Important Polymers

21. Robert AD (1998) Natural Rubber Science and Technology. Oxford University Press

22. Kosugi K, Sutthangkul R, Chaikumpollert O, Yamamoto Y, Sakdapipanich J, Isono Y, Kawahara S (2012) Preparation and characterization of natural rubber with soft nanomatrix structure. Colloid Polym Sci 290:1457–1462